Scanning pentaprism measurements of off-axis aspherics II

Peng Su[a] , James H. Burge[a, b], Brian Cuerden[b], Richard Allen[b], Hubert M. Martin[b]

[a]College of Optical Sciences, the University of Arizona, Tucson, AZ 85721,U.S.A.
[b]Dept.of Astronomy/Steward Observatory, the Univ. of Arizona, Tucson, AZ 85721, U.S.A

ABSTRACT

The scanning pentaprism test has provided an important absolute test method for flat mirrors, parabolic mirrors and also collimation systems. We have developed a scanning pentaprism system to measure off-axis paraboloidal mirrors such as those for the Giant Magellan Telescope (GMT) primary mirror. Special characteristics of the pentaprism testing of an off-axis mirror are discussed in the paper. We provide performance results for the final measurement of a 1.7 m off-axis parabolic mirror and present a technique used to determine the radius of the parent, off-axis distance and the clocking of the mirror from the data from the scanning pentaprism system.

Keywords: Aspherics, telescope, optical testing

1. INTRODUCTION

The scanning pentaprism test has provided an important absolute test method for flat mirrors, for parabolic mirrors and also for collimation systems[1, 2]. The pentaprism test of off-axis aspherics utilizes the property of a paraboloidal or near paraboloidal surface where all rays parallel to the optical axis will go through or near its focal point. However, for off-axis aspherics, different from measuring flat mirrors or rotationally symmetric surfaces, data collection and reduction parts of the scanning pentaprism test have to be modified and specialized for accommodating the situation of broken rotational symmetry and field aberration issue. These have been partially discussed in our former paper[3]. Here we will provide further discussions. The 1.7 meter New Solar Telescope (NST) primary mirror, which is close to a 1/5 scale of the GMT off-axis segment, was tested recently with the scanning pentaprism method when the mirror was finished, allowing an excellent assessment of the performance of the pentaprism system. We also present the analysis used to determine the radius of the parent, off-axis distance and clocking of the mirror.

2. SCANNING PENTAPRISM SYSTEM

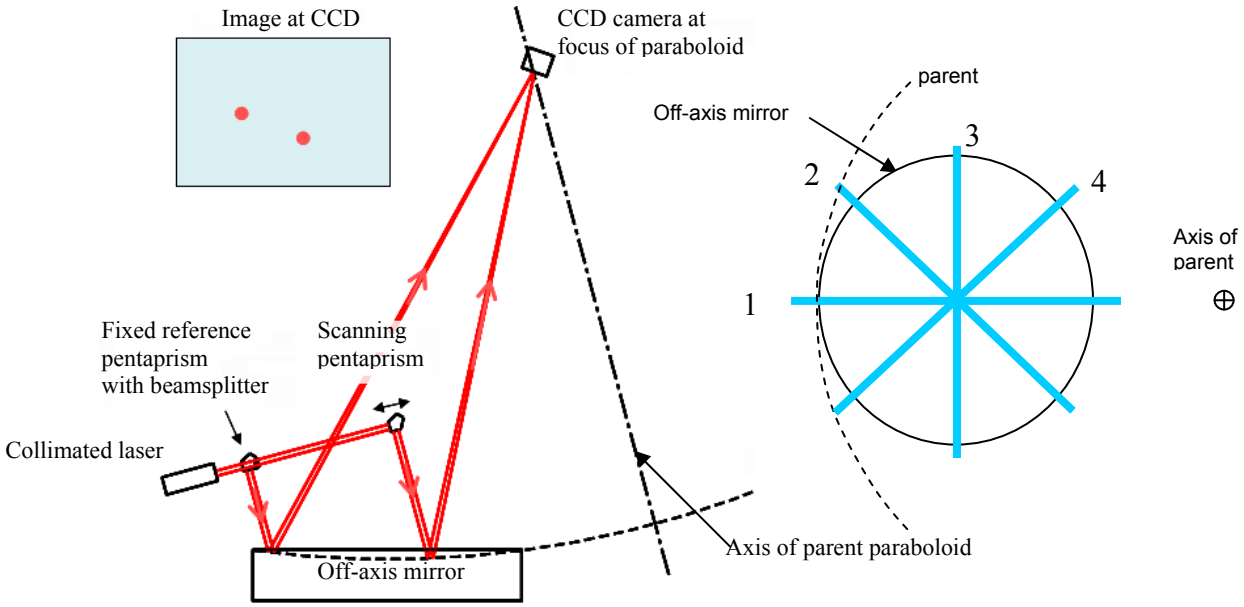

Figure 1. Basic principle of the scanning pentaprism test (left), scanning pattern as viewed from projection along parent axis (right)

Optical Manufacturing and Testing VIII, edited by James H. Burge, Oliver W. Fähnle, Ray Williamson,
Proc. of SPIE Vol. 7426, 74260Y · © 2009 SPIE · CCC code: 0277-786X/09/$18 · doi: 10.1117/12.828497

2.1 NST Scanning Pentaprism System

The NST mirror is a 1.7m diameter off-axis parabola (OAP), with a 1.84 m off -axis distance. The vertex radius of curvature of its parent is 7700 mm. Four pentaprism scans were used to measure the mirror as shown in Fig.1. The displacement of the spot at the focal plane, as a function of position in the pupil, gives a measurement of the surface slope errors. By integrating the slope data, or fitting polynomials to them, the surface shape can be obtained.

The NST scanning pentaprism assembly (SPA) uses two pentaprisms on a rail. A collimated light source (beam projector) projects light along the rail. One pentaprism with beam splitter is located at one end of the rail. The other pentaprism can be positioned at any point along the rail using a motor control. The pentaprisms deviate light by 90 degrees, independent of small tilts in the prism itself. The NST mirror focuses these beams to two spots in the focal plane of the mirror. A CCD detector is located there to capture spot images. An example image is shown in Fig. 2 (a). A correlation method[4] is then used to calculate the centers of the spots. With two pentaprisms, motion of the beam projector can be removed by measuring the differential motion. Fig. 2 (b) shows our scanning pentaprism test setup. The pentaprism rail carrying the beam projector and two prisms can sit at four different locations on a supporting frame to realize the four measurement scans. To minimize the pentaprism second order effects[2] from its yaw and roll, an electronic autocollimator is used to monitor yaw of the scanning prism, then the yaw errors are compensated in real time by adjusting the yaw of the prism electronically. The roll of the prism is monitored in the detector plane and is corrected with another actuator.

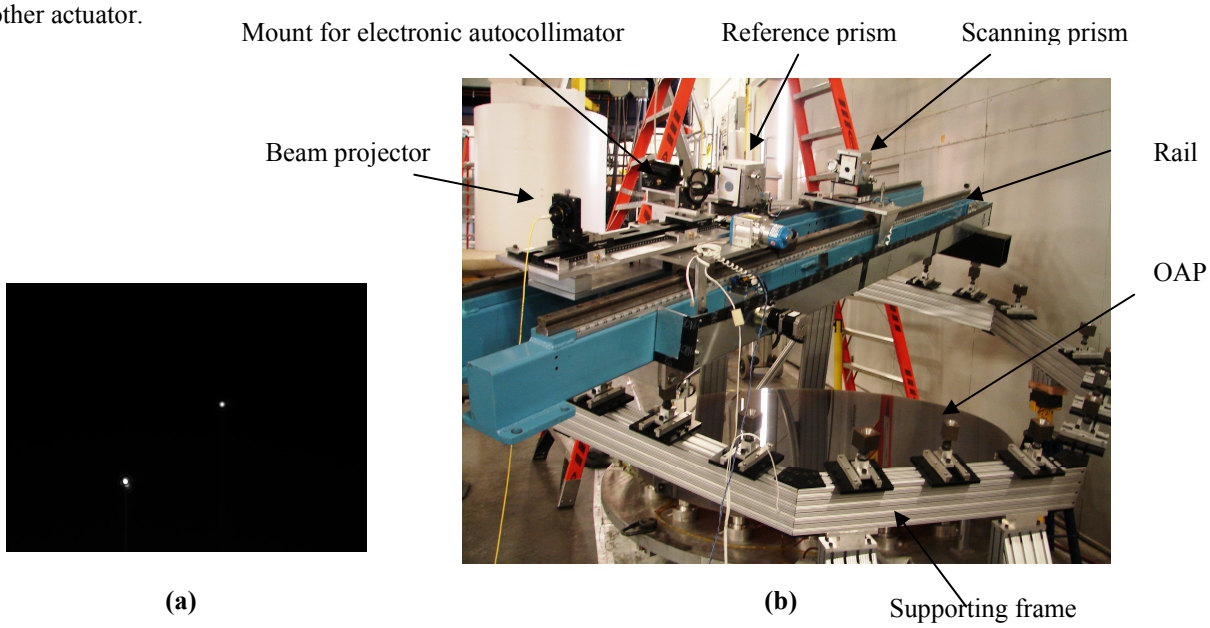

Fig.2. (a) Image of the spots at focal plane of the mirror, (b) Scanning pentaprism system test setup(CCD detector is mounted at focal plane of the OAP, ~4m above this setup, not shown in the figure)

2.2 Testing of Off-axis Aspherics: Field Aberration Effect

The pentaprism test for an off-axis parabola has some special characteristics when compared with the test for a flat mirror or rotationally symmetric surface.

2.2.1. All scans need to be collected from the same field of view or a known field relationship between scans

If a parabolic mirror is illuminated with collimated light that is parallel to its axis, all reflected rays go through the focal point of the parabola. If these rays are not parallel to the axis, illuminated at an angle, the rays will shift away from the focal point and they no longer intersect at a point. For a full axially symmetric mirror, this effect is described as Seidel coma. The off axis portion simply samples this, which appears as a combination of astigmatism, coma and trefoil in the wavefront. The magnitude of this aberration is linear with the misalignment. Fig. 3 shows simulated field aberration

wavefront maps given ±0.001° incident beam angles in two orthogonal directions, *y* and *x*, which are the directions in the plane of symmetry of the mirror and the perpendicular direction.

When the fabricated mirror is mounted to the telescope, mirror position (changing field) is also used as a degree of freedom to compensate for the errors in the mirror surface, because field aberration can cancel astigmatism and coma in the mirror surface itself. So an error budget for the mirror segment which is a combination of the surface error and mirror movement (field) was defined for fabrication. During the alignment of the scanning pentaprism test, field aberrations need to be aligned or known to within a certain tolerance. Since there are field aberrations in the test, measurements from the same field of view are needed during the four scans, otherwise random field aberrations will be introduced to the different scans. This was done by aligning the SPA to focus the light to the same pixel in the detector plane for the common intersection point of the four scans. During the data reduction, field aberration components can be fitted and removed from surface estimate.

$$Z5 = \sqrt{6}\rho^2 \sin(2\theta) \qquad Z7 = \sqrt{8}(3\rho^3 - 2\rho)\sin(\theta) \qquad Z9 = \sqrt{8}\rho^3 \sin(3\theta)$$

$$Z6 = \sqrt{6}\rho^2 \cos(2\theta) \qquad Z8 = \sqrt{8}(3\rho^3 - 2\rho)\cos(\theta) \qquad Z10 = \sqrt{8}\rho^3 \cos(3\theta)$$

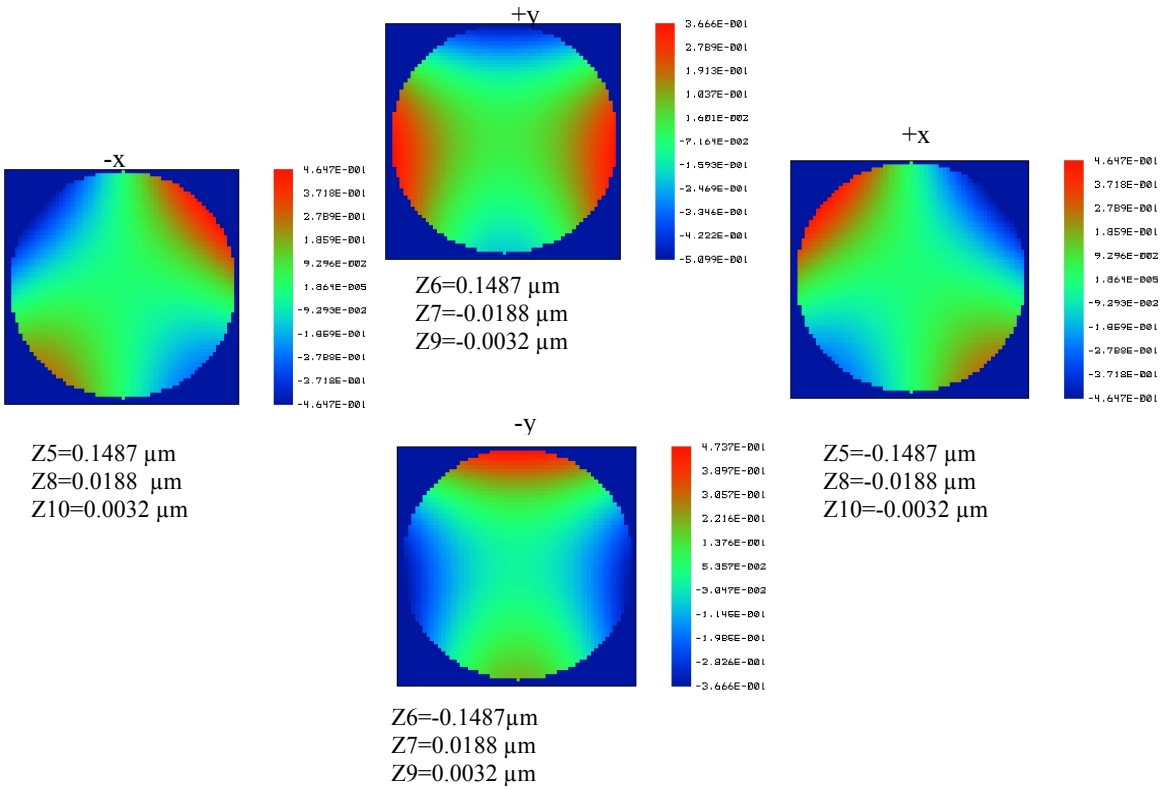

Fig. 3. Wave aberrations due to 0.001° field of view and their Zernike coefficients

2.2.2 In-scan and cross-scan directions vary with pupil position

As shown in the right of Fig 1, three of the four scans no longer pass toward the center of the parent axis of the mirror. Plane symmetry is not available for scans 2, 3 and 4. Moreover, as an off-axis part of a parabolic surface, the mirror suffers field aberrations when the SPA is not perfectly aligned to the mirror. Because of the two features mentioned above, the in-scan (corresponding prism pitch direction in detector plane) and cross-scan directions (corresponding spot motion direction in detector plane due to prism roll and yaw) of the pentaprism test in the detector plane change orientations at different pupil locations during a single scan. An intuitive way to understand this is shown in Fig. 4. A

cross-scan motion would introduce a field angle. In the figure, the red spots correspond to scan 3 in Fig.1 right. Fig. 4 shows that as the field changes linearly, which represents pentaprism roll and yaw, the pattern of the field error would be linearly shifted and scaled. Connecting the spots from the same position on the mirror surface with lines, one can see that the cross scan directions in the focal plane are changing at different positions of the mirror due to the field aberration. Mathematical explanation of this effect can be found in Ref. 6.

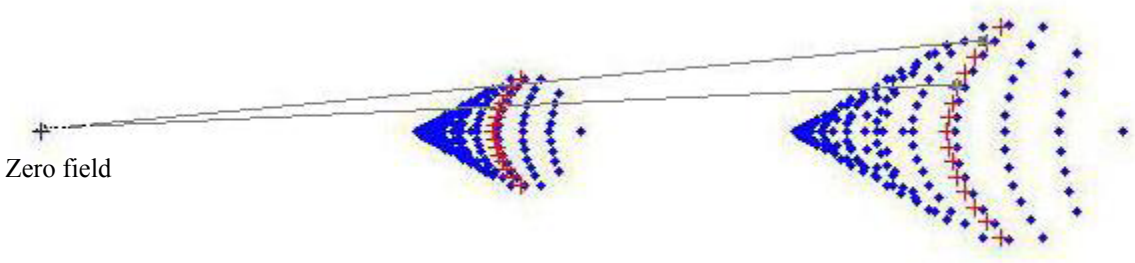

Fig. 4. Field (cross-scan spot motion) will linearly shift and scale the spot diagram. The cross-scan direction is changed at different pupil positions in a single scan.

2.2.3 The spot motions from static and scanning prisms are no longer the same due to the field effect

Due to the field effect, the spot motions from static and scanning prisms are no longer the same but have a predictable relationship. The magnitude of the field aberrations is a function of position in the pupil. This causes the static spot and the scanning spot to have different amount of motions when the beam projector changes in pitch, since the two beams from the pentaprisms sample different pupil positions. This effect was simulated with a ray tracing program. The motion scale factors between the static spot and the scanning spot were calculated. Fig. 5 shows the scale factors for the zero degree scan. Data were normalized to the value of the reference spot (point 1). As shown in the figure, the movement of the other sample point due to the pitch of the beam projector can be obtained by multiplying the in-scan motion of the static spot by its scale factor. Then this in-scan motion from beam projector pitch can be removed from the prism data. We calculated the scale factors for all the scans and checked them in the experiment by tilting the rail and measuring the spot motions. The prediction from the model matched the experimental data very well.

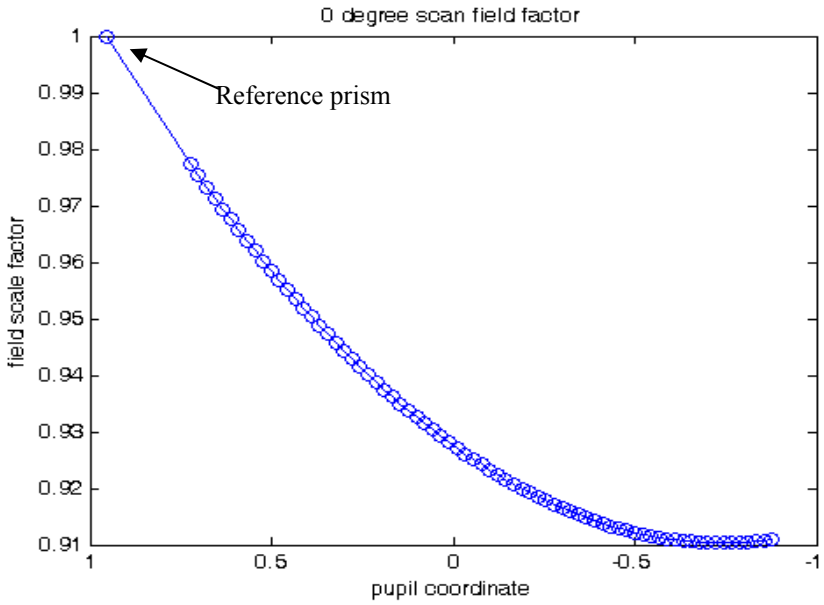

Fig. 5. Field effect correction factors for the 0° scan, normalized to the reference prism.

3. TEST RESULT FOR THE NST OAP

3.1 Surface Figure Test Result

The previous paper [3] showed the scanning pentaprism measurement results for the NST mirror before the mirror was finished. Fig. 6 shows the comparison between the pentaprism test (four scans and 37points/scan) and interferometric test using a computer generated hologram (CGH) at the center of curvature of the mirror.

In Figures 7 and 8, we give the pentaprism test results when the mirror was finished. Four scans were taken as the pattern shown in Fig. 1 right. Seventy-three points were sampled during each scan to resolve most of the high-spatial-frequency slope errors. Fig. 7 shows the spot diagrams obtained from the different scans, including focus error left in the alignment. Fig.8 shows the residuals after the polynomial fit was removed[3]. Table 1 lists the coefficients of the fit from the pentaprism test and coefficients obtained from the interferometric null test.

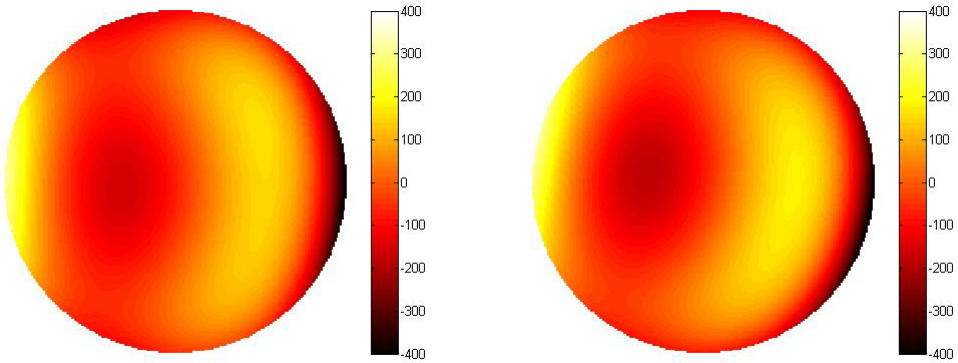

Fig. 6. Surface estimate from the pentaprism test and an interferometric test before the mirror was finished. Color bar is labeled in nm of surface error.

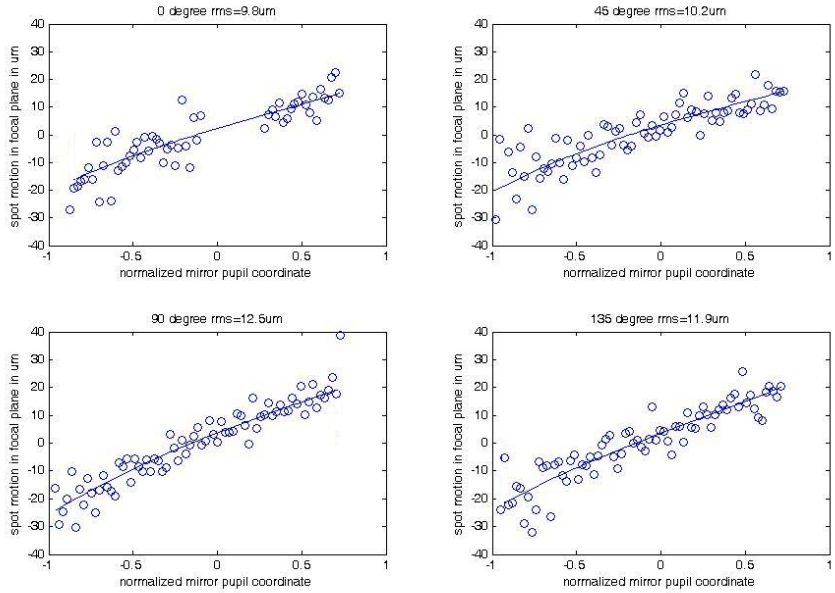

Fig. 7. Spot motion in focal plane vs. mirror pupil coordinate. Focus alignment error accounts for the common linear motion.

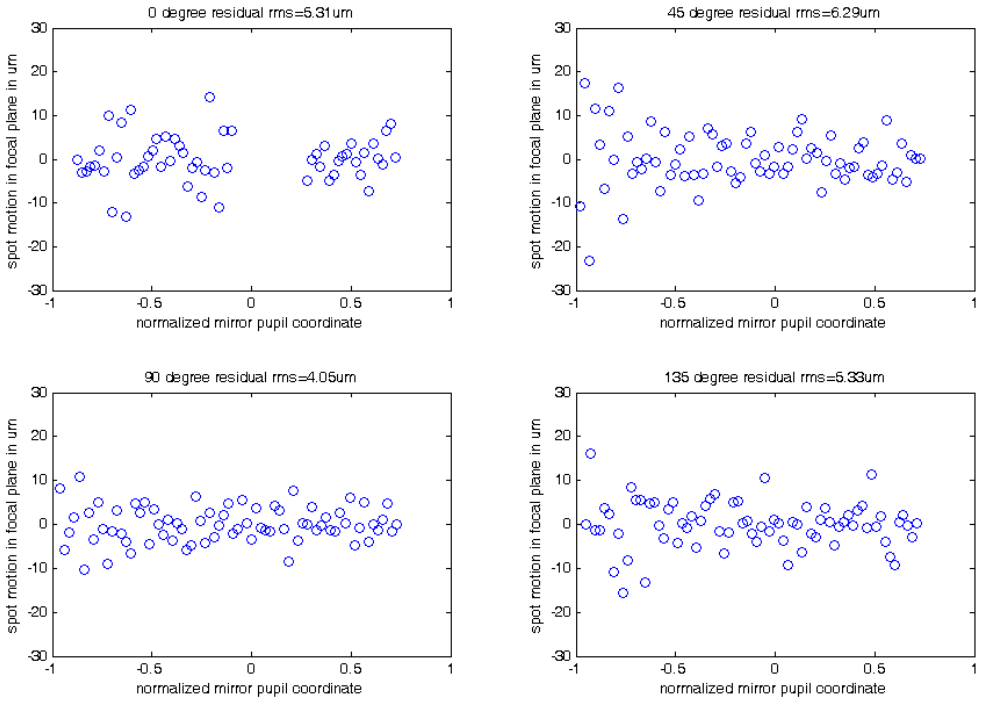

Fig. 8. Fitting residuals of each scan

Table 1. Surface coefficients from pentaprism test and interferometric test. Astigmatisms are much smaller than the uncertainty because certain combinations of astigmatism and coma (field aberration) have been removed from the final figure estimate.

aberration	interferometer nm rms surface	pentaprism nm rms surface
astigmatism 0°	1	-1 ±16
astigmatism 45°	0	0 ±16
coma 0°	1	0 ±7
coma 90°	-4	8 ±7
trefoil 0°	-1	-8 ±19
trefoil 30°	-2	-3 ±19
spherical	-1	-4 ±5
RSS	5	12

Summary of the test errors

Considering different error sources as discussed in reference 3, 1 μrad rms wavefront slope error was set as the test error budget, which gives a total surface measurement uncertainty less than 38 nm rms for 73points/scan and a total of 4 scans. Tables 2 and 3 summarize the errors contributed by different sources. Detailed error analysis can be found in Ref. 6.

Table 2. Errors described by slope changes [3]

	Scanning prisms (μrad *rms*)	Explanation
Determination of image position	0.52	2 μm *rms* for each spot in focal plane
High frequency surface residuals	0.64	Treating the high-frequency data from interferometric measurement as random errors
Phase errors in beam projector; coupling of diffraction effects with lateral motion; beam non-uniformity	negligible	
Motion and misalignment	0.26	Roll and yaw effects
RSS	0.86 (32 nm rms surface error, 73points/scans)	

Table 3. Errors described by surface rms

	Rms surface error (nm)	Explanation
Error due to field variation	1.5	±1.6 urad field difference between scans
Error due to focus variation	4.7	±3 μm focus difference between scans
RSS	5	

3.2 Determination of Mirror focal length, Off-axis Distance and Clocking Angle

The ability to combine the CCD data in pixels (image spot position) with laser tracker data of mirror position provides a way to determine focal length and other geometric parameters of the mirror.

To get the coordinate relation between the mirror and the CCD detector, a laser tracker is used for coordinate measurements[5]. Mirror coordinates are obtained by directly touching the mirror with the tracker ball. The tracker ball data are further corrected to get the coordinates of the surface contacting points. For CCD detector coordinates, three laser tracker balls are attached to the mount of the detector. Detector coordinates are determined by calibrating the tracker ball locations relative to the detector pixels. During the test, for all scans, the rail was adjusted to focus the light to the same pixel in the detector, which corresponds to a certain field of view of the mirror. In data reduction, the alignment information including the field aberration (field angle) and focus can be obtained from the data fitting [6]. The focus of the mirror in space can then be determined from the detector pixel position and alignment information. With laser tracker data of the mirror, focal length, off-axis distance and clocking angle can be calculated based on the equal optical path method as described below.

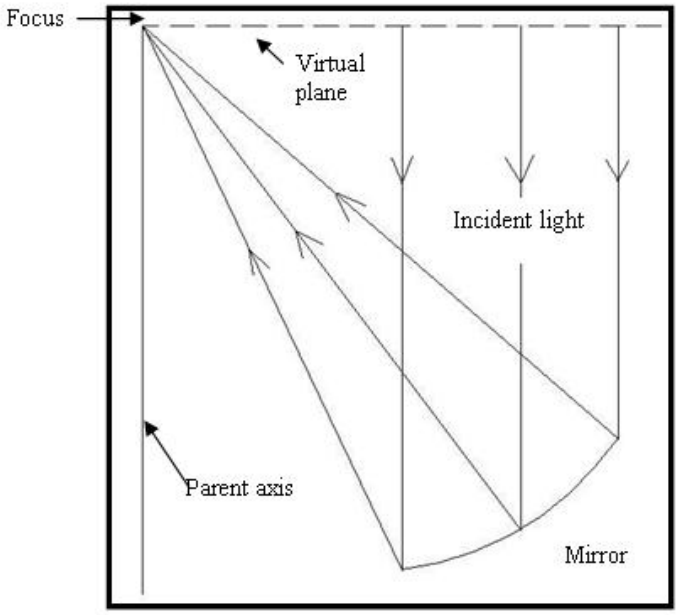

Fig. 9. Principle of the equal optical path method for determining mirror geometric parameters

Knowing mirror surface data and the focus of the mirror, the equal optical path method is used to find the direction of the parent axis, which determines the geometry of the mirror. This is done by optimizing the direction of the parent axis until the different optical paths calculated from the focal point and points on the mirror are equal; this is the defining property of a parabola. After getting the direction of the parent axis in the mirror coordinate system, the mirror geometry can be calculated directly.

Fig. 9 shows the coordinate relations between the points on the mirror and the focus of the mirror. For on-axis light, the incident light is parallel to the parent axis. A virtual plane passing through the focus of the mirror and perpendicular to its parent axis can be drawn as the dashed line shown in the figure. This plane also intercepts the incident light at different points. The incident light is perpendicular to the virtual plane. For a parabolic surface, different rays should have the same optical path from the virtual plane to the focus of the mirror. So the direction of the parent axis can be optimized to satisfy this requirement. Half of the above optical path gives the focal length of the parent mirror. The distance between the mirror center and the parent axis gives the off-axis distance of the mirror. With the direction of the parent axis and the coordinates of the clocking reference marks on the mirror, the clocking angle of the mirror can then be calculated. A Monte Carlo simulation was done with a 0.1mm uncertainty of the focus and 20 μm uncertainties of the coordinates on the mirror. A focal length uncertainty of less than 0.4 mm and an off-axis distance uncertainty of less than 1 mm were obtained. Table 4 shows the mirror geometry data obtained from equal path method and the interferometric test. Detailed data reduction and analysis are shown in Ref. 6.

Table 4. Mirror geometry data from pentaprism test and interferometric test

Mirror geometry	Focal length of the parent	Off-axis distance	Clocking angle
Measure from pentaprism test	3849.9±0.4 mm	1838.7±1mm	0.023°
Measure from interferometric test	3849.6±0.5 mm	1840.6±1mm	0.006°

4. SUMMARY

The scanning pentaprism test has been successfully applied to measure flat and rotationally symmetric curved mirrors. Our work applied it to measure off-axis surfaces which suffer significant amounts of field aberrations when the test

system is not perfectly aligned. Field aberrations induce changes in the direction of the in-scan and cross-scan spot motion during a single scan. All the scan data should be collected at the same field of view or with a known relationship. Also, due to the field effect, spot motions from the static and scanning prisms are no longer the same but have a predictable relationship. All these effects are now understood and solved experimentally and mathematically in our test. Moreover, we also showed how to use the pentaprism test data to calculate the geometric parameters of the mirror. The scanning pentaprism test is one of the verification tests for the GMT mirror. In that case, the surface is not exactly a parabola, so the test will be a non-null test; however, the basic principle has been demonstrated in the NST test.

REFERENCES

[1] James H. Burge, *Advanced Techniques for Measuring Primary Mirrors for Astronomical Telescopes*, Ph.D. Dissertation, Optical Sciences, University of Arizona (1993).

[2] Jullius Yellowhair, Peng Su, Matt Novak, James H. Burge, "Fabrication and Testing of Large Flats," Proc. of SPIE Vol.6671, 667107 (2007).

[3] Peng Su, James H. Burge, Brian Cuerden, Jose Sasian, Hubert M. Martin, "Scanning pentaprism measurements of off-axis aspherics," Proc. SPIE 7018, 7018 3T (2008).

[4] Prateek Jain, "Hartman Spot Position Sensing," internal technical memo (June 2002).

[5] James H. Burge, Peng Su, Chunyu Zhao, Tom Zobrist, "Use of a commercial laser tracker for optical alignment," Proc. SPIE 6676, 66760E (2007).

[6] Peng Su, James H. Burge, Hubert M. Martin, "Scanning pentaprism measurements of off-axis parabola," to be submitted to Appl.Opt. (2009).